International Journal of Control and Automation
Vol. 8, No. 1 (2015), pp. 197-210
http://dx.doi.org/10.14257/ijca.2015.8.1.18

Study on Series Control Method for Dual Three-Phase PMSM based on Space Vector Pulse Width Modulation

Huaqiang Zhang[1], Shijun Luo[1], Yaxin Yu[1]and Lingshun Liu[2]
[1]Department of Electrical Engineering, Harbin Institute of Technology at Weihai, Weihai Shandong 264209, China
[2]Department of Control Engineering, Naval Aeronautical and Astronautical University, Yantai Shandong 264001, China
zhq@hit.edu.cn; luoshijun101001@163.com; yyxjane@163.com; lingshunliu@sohu.com

Abstract

Decoupling control of two-motor dual three-phase permanent-magnet synchronous motor (PMSM) series-connected system can be realized by using proper phase transposition rules with a single supply from a six-phase voltage source inverter (VSI), which solved the control problem of two motors in series. Since the traditional two-vector SVPWM strategy, which is commonly used in three-phase system, exists 5th and 7th harmonics in x-y plane, making it hard to realize decoupling control of two-motor dual three-phase PMSM series-connected system. Meanwhile, the DC bus voltage utilization of carrier-based PWM strategy is lower. Thus one method, which adopted a TBTSB-SVPWM strategy with two modulators, was proposed in this paper. It ensures the inverter output voltage only contains two kinds of fundamental components required by the two series-connected motors with a single VSI, making it possible to realize decoupling control of two-motor dual three-phase PMSM series-connected system. Simulation results indicate that there is no influence on the other motor while the speed/load of any one motor changed, achieving the decoupling control of series-connected system, and the feasibility and validness of the proposed approach are verified.

Keywords: *Dual three-phase permanent-magnet synchronous motor; series-connected system; space vector pulse width modulation; single inverter; decoupling control*

1. Introduction

In electric ship propulsion system, more-electric aircraft drive system and locomotive traction system [1-16], multiple motors are always required to operate independently under different working conditions. In general case, one motor works at low-speed/high-torque condition, while the other motor operates at high-speed/low-torque condition. Currently, there are mainly two types of multi-motor systems. The first one, each motor is independently drove by individual inverter sharing the same DC bus. In such a system all motors are permitted to have different rated parameters, speeds and torques. However using multiple inverters greatly increases the volume and cost of the drive system. The second one is multi-motor parallel-connected system with a single supply from a multiphase VSI. In order to control all motors in parallel independently, the same phase-transposition rules used in series system, are also adopted in parallel system. However, the parallel-connected system suffers some serious disadvantages compared with series-connected system [2]. First, the phase number of each motor in parallel system must be equal to the phase number of inverter, while in series system with a single VSI, motors with different phase number can be connected in series, for example, an asymmetric six-phase motor is connected with a two-phase motor. In addition, the most serious problem

ISSN: 2005-4297 IJCA
Copyright ⓒ 2015 SERSC

of parallel-connected system is lack of control over *x*-*y* current components. Since these current components are determined by the *x*-*y* plane voltage reference vector and the small impedance of other motor. The values of them are always very high. In conclusion, it is very hard to realize independent control of motors in parallel system in the real world application.

According to the theory of vector control, any n-phase motor can be controlled by using only two current components (one is torque current and the other is excitation current) in the rotating reference frame. With the increasing of phase number, redundancy current components existing in multi-phase motor can be used to control another machine. So far, some foreign scholars are mainly concentrating on the study of two-motor five-phase induction motor series-connected system with a single VSI. However, there has been little study into the two-motor dual three-phase PMSM series-connected system with a single VSI.

Phase transposition rules of series-connected system and modeling of multiphase motor are elaborated in [5-7]. For the purpose of pure sinusoidal output phase voltage and improving DC bus voltage utilization, the SVPWM technique of five-phase induction motor, six-phase induction motor and seven-phase induction motor are detailed in [8]-[13]. In [3,4, 13-16], current hysteresis control, current ramp-comparison control and SVPWM control are used to realize independent decoupling control for the two-motor five-phase induction motor series-connected system with a single VSI. This paper mainly studied the two-motor dual three-phase PMSM series-connected system. Simulation experiments of two-motor dual three-phase PMSM series-connected system are performed in Matlab/Simulink, based on a TBTSB-SVPWM (Two biggest and two second-biggest space vector pulse width modulation) technique, in conjunction with i_d=0 vector control strategy, and finally the feasibility and validness of the proposed approach are verified.

2. Series Control of Dual Three-Phase PMSM

2.1. Theoretical Analysis of Series-Connected system

Stator windings of dual three-phase PMSM consist of two sets of three-phase windings, which are spatially shifted by 30^o electrical degree. The first set is *abc*, the second set is *xyz*, and the load is star-connected with isolated neutral point. The two-motor dual three-phase PMSM series-connected system is illustrated in Figure 1. It can be seen from Figure 1 that the phase transposition rules of two-motor dual three-phase PMSM series-connected system are as follows: a_1-a_2, x_1-y_2, b_1-c_2, y_1-x_2, c_1-b_2, z_1-z_2.

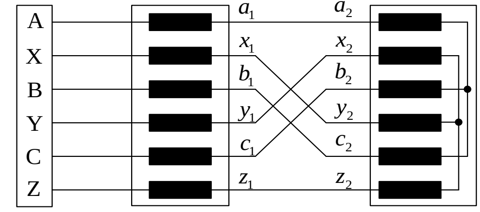

Figure 1. Two-motor Dual Three-phase PMSM Series-connected System

Take current variables for example, the independent decoupling control theory of two-motor dual three-phase PMSM series-connected system is elaborated next. Assume that the inverter output phase currents are denoted by i_A, i_B, i_C, i_X, i_Y, i_Z. Each phase current contains two fundamental components with different amplitudes and frequencies, required by the two series-connected motors respectively. Where I_{m1} and I_{m2} represent phase-current fundamental RMS of motor1 and motor2 respectively, simultaneously ω_1 and ω_2 represent phase-current fundamental frequency of motor1 and motor2 respectively.

$$\begin{bmatrix} i_{\mathrm{A}} \\ i_{\mathrm{B}} \\ i_{\mathrm{C}} \\ i_{\mathrm{X}} \\ i_{\mathrm{Y}} \\ i_{\mathrm{Z}} \end{bmatrix} = \begin{bmatrix} \cos\omega_1 t & \cos\omega_2 t \\ \cos(\omega_1 t-4\alpha) & \cos(\omega_2 t-8\alpha) \\ \cos(\omega_1 t-8\alpha) & \cos(\omega_2 t-4\alpha) \\ \cos(\omega_1 t-\alpha) & \cos(\omega_2 t-5\alpha) \\ \cos(\omega_1 t-5\alpha) & \cos(\omega_2 t-\alpha) \\ \cos(\omega_1 t-9\alpha) & \cos(\omega_2 t-9\alpha) \end{bmatrix} \begin{bmatrix} \sqrt{2} I_{\mathrm{m1}} \\ \sqrt{2} I_{\mathrm{m2}} \end{bmatrix} \tag{1}$$

After decoupling transformation, expression (1) is translated into expression (2).

$$\begin{bmatrix} i_\alpha \\ i_\beta \\ i_x \\ i_y \\ i_{o1} \\ i_{o2} \end{bmatrix} = [\mathbf{C}_{6\mathrm{s}/2\mathrm{s}}] \begin{bmatrix} i_{\mathrm{A}} \\ i_{\mathrm{B}} \\ i_{\mathrm{C}} \\ i_{\mathrm{X}} \\ i_{\mathrm{Y}} \\ i_{\mathrm{Z}} \end{bmatrix} = \begin{bmatrix} \sqrt{3} I_{\mathrm{m1}} \cos\omega_1 t \\ \sqrt{3} I_{\mathrm{m1}} \sin\omega_1 t \\ \sqrt{3} I_{\mathrm{m2}} \cos\omega_2 t \\ \sqrt{3} I_{\mathrm{m2}} \sin\omega_2 t \\ 0 \\ 0 \end{bmatrix} \tag{2}$$

$$\mathbf{C}_{6s/2s} = \sqrt{\frac{1}{3}} \begin{bmatrix} 1 & \cos 4\alpha & \cos 8\alpha & \cos\alpha & \cos 5\alpha & \cos 9\alpha \\ 0 & \sin 4\alpha & \sin 8\alpha & \sin\alpha & \sin 5\alpha & \sin 9\alpha \\ 1 & \cos 8\alpha & \cos 4\alpha & \cos 5\alpha & \cos\alpha & \cos 9\alpha \\ 0 & \sin 8\alpha & \sin 4\alpha & \sin 5\alpha & \sin\alpha & \sin 9\alpha \\ 1 & 1 & 1 & 0 & 0 & 0 \\ 0 & 0 & 0 & 1 & 1 & 1 \end{bmatrix} \tag{3}$$

Where $\mathbf{C}_{6\mathrm{s}/2\mathrm{s}}$ denotes the decoupling transformation matrix given with the expression (3) and $\alpha=30^{\mathrm{o}}$. The first two rows represent current components in α-β plane; the middle two rows represent current components in x-y plane and the last two rows represent zero-sequence components.

It can be seen from expression (2), different frequency and amplitude phase current fundamental components, required by individual motor, are mapped into two 2-D planes (α-β plane and x-y plane). In series-connected system, α-β current components are used to control motor1, while x-y current components are used to control motor2. Since α-β plane and x-y plane are orthogonal without mutual coupling, thus it is possible to control the two series-connected motors independently.

It must be noted that the above analysis is based on the fact that the phase voltage is pure sinusoidal. However, the inverter output voltage always contains some harmonics, which makes it hard to realize decoupling control of series-connected system. Thus it is necessary to study the influence of harmonics on series-connected system.

2.2. Harmonics Influence

According to coordinate transformation theory, the mathematical model of dual three-phase PMSM in natural coordinates can be decoupled by decoupling transformation matrix and mapped into three orthogonal planes (α-β plane, x-y plane and o_1-o_2 plane). The fundamental and harmonics of the order $6k\pm1$ (k=2, 4, 6…) are mapped into α-β plane, which generate the rotating magnetic field and participate in electromechanical energy conversion. Harmonics of the order $6k\pm1$ (k=1, 3, 5…) are mapped into x-y plane, which do not contribute to flux production and have no correlation with electromechanical energy conversion, and are commonly referred as generalized zero-sequence components. While harmonics of the order $3k$ (k=1, 2, 3…) are mapped into o_1-o_2 plane, which do not exist in star-connected multiphase system, and are commonly referred as zero-sequence components [17-20].

For the two-motor dual three-phase PMSM series-connected system, since motor1 operates on the *α*-*β* plane, while the 6*k*±1 (*k*=1, 3, 5…) order harmonics of motor2 are mapped into *α*-*β* plane, which lead to flux production and cause torque ripple in motor1, thus motor1 can't operate stably. Similarly, since motor2 operates on the *x*-*y* plane, while the 6*k*±1 (*k*=1, 3, 5…) order harmonics of motor1 are mapped into *x*-*y* plane, which lead to flux production and cause torque ripple in motor2, thus motor2 can't operate stably.

In order to realize decoupling control of two dual three-phase PMSM series-connected system, it is important to ensure that the inverter output voltage only contains two kinds of fundamental components required by each motor.

2.3. Control Strategy of Series-Connected System

The two-motor dual three-phase PMSM series-connected system is depicted in Figure 2. The vector control strategy based on $i_{\mathrm{d}} = 0$ is adopted in this paper. Through SVPWM modulator, proper switching signals can be obtained and the inverter generates two kinds of phase voltage fundamental components required by the two series-connected motors respectively. In Figure 2, ω_{m1}^{*} , ω_{m2}^{*} and ω_{m1} , ω_{m2} are given angular velocity and feedback angular velocity of motor1 and motor2 respectively; i_{d}^{*} , i_{z1}^{*} and i_{d} , i_{z1} are given current and feedback current in d-axis of motor1 and motor2 respectively; i_{q}^{*} , i_{z2}^{*} and i_{q} , i_{z2} are given current and feedback current in q-axis of motor1 and motor2 respectively; θ_{e1} and θ_{e2} are rotor position of motor1 and motor2.

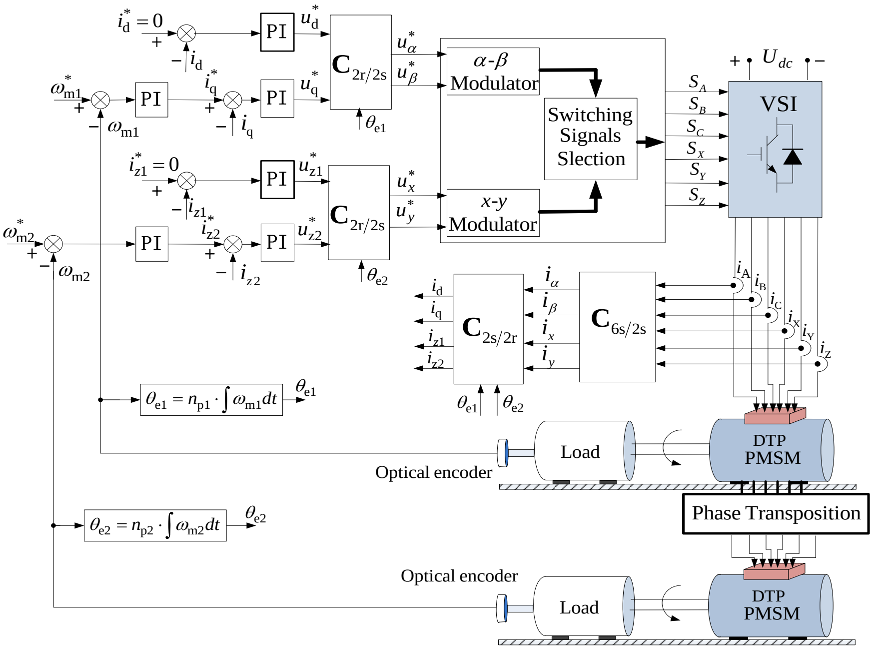

Figure 2. Two-motor Series-connected System of Dual Three-phase PMSM

In order to make inverter output phase voltage only contains two kinds of sinusoidal fundamental components with different frequencies and amplitudes, and after decoupling transformation of the inverter output phase voltage, and these two kinds of fundamental components could be mapped into *α*-*β* plane and *x*-*y* plane respectively. It is required that the modulator in *α*-*β* plane only generates *α*-*β* reference voltage vector, and makes *x*-*y* reference voltage vector be equal to zero simultaneously. Similarly, the modulator in *x*-*y* plane only generates *x*-*y* reference voltage vector, and makes the *α*-*β* reference voltage vector be equal to zero.

Copyright ⓒ 2015 SERSC

Since the traditional SVPWM technique only takes *α-β* reference voltage vector into consideration, and lacks control over the *x-y* reference voltage vector, thus 5th and 7th harmonics are generated in phase voltage, making it impossible to realize decoupling control of series-connected system. In fact, the reference voltage vector of the dual three-phase PMSM is a 4-D vector, so four basic space voltage vectors at least are required to control it completely. Thus the following control strategy was adopted in this paper, as is showed in Figure 3. Assume that the inverter switching period is T_s. According to the volt-second balance theorem, in the first switching period, *α-β* reference voltage vector is synthesized by selecting a set of four basic space voltage vectors (two biggest and two second biggest basic space voltage vectors) in *α-β* plane. In the next switching period, the *x-y* reference voltage vector is synthesized by selecting a set of four basic space voltage vectors (two biggest and two second biggest basic space voltage vectors) in *x-y* plane. The selection of switching signals is depicted in Figure 3. It indicates that this SVPWM method consists of two modulators (*α-β* modulator is used to control motor1, and *x-y* modulator is used to control motor2).

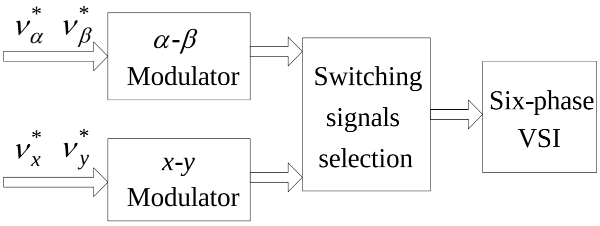

Figure 3. The Selection of Inverter Switching Signals

3. SVPWM Technique of Series Connected System

3.1. Distribution of Basic Space Voltage Vectors

The six-phase VSI is illustrated in Figure 4. Phase voltages of motor are denoted by lowercase letters (a, b, c, x, y, z), while the inverter leg voltages are denoted by capital letters (A, B, C, X, Y, Z). The relationship between motor phase voltages and the inverter leg voltages can be described as expression (4).

$$\begin{aligned}
v_a &= 2/3 v_{AO} - 1/3(v_{BO} + v_{CO}) \\
v_b &= 2/3 v_{BO} - 1/3(v_{AO} + v_{CO}) \\
v_c &= 2/3 v_{CO} - 1/3(v_{AO} + v_{BO}) \\
v_x &= 2/3 v_{XO} - 1/3(v_{YO} + v_{ZO}) \\
v_y &= 2/3 v_{YO} - 1/3(v_{XO} + v_{ZO}) \\
v_z &= 2/3 v_{ZO} - 1/3(v_{XO} + v_{YO})
\end{aligned} \tag{4}$$

Where the inverter leg voltage v_{kO} (k=A, B, C, X, Y, Z) takes the values of ±0.5U_{dc}.

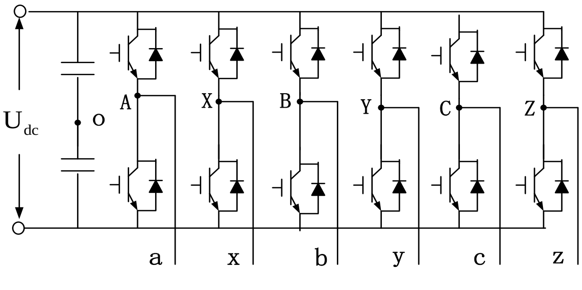

Figure 4. The Topology of a Six-phase Voltage Source Inverter

In general, an n-phase two-level VSI has a total of 2^n basic space voltage vectors. Thus in the case of six-phase VSI, there are 64 basic space voltage vectors, 60 of which are nonzero space voltage vectors and 4 of which are zero space voltage vectors. Each switching state of inverter can be denoted by a set of octal numbers, for example, the subscript of space voltage vector v_{44} can be described as ABCXYZ=100100, which indicates that the upper switch of A-phase and X-phase are “on”, and the lower switch of A-phase and X-phase are “off”; simultaneously the upper switch of B-phase, C-phase, Y-phase, Z-phase are “off”, and the lower switch of B-phase, C-phase, Y-phase, Z-phase are “on”. In conjunction with expression (4) and expression (5), it is easy to calculate all basic space voltage vectors corresponding to the inverter switching states. All basic space voltage vectors in *α-β* plane and in *x-y* plane are showed in Figure 5. It can be seen from Figure 5 that the biggest amplitude space voltage vectors in *α-β* plane are mapped into the smallest amplitude space voltage vectors in *x-y* plane, and the smallest amplitude space voltage vectors in *α-β* plane are mapped into the biggest amplitude space voltage vectors in *x-y* plane, while the amplitudes of the remaining basic space voltage vectors keep unchanged both in *α-β* plane and in *x-y* plane.

$$\begin{aligned} v_{\alpha\beta} &= v_\alpha + jv_\beta = 1/3\,(v_a + v_x e^{j30^\circ} + v_b e^{j120^\circ} \\ &\quad + v_y e^{j150^\circ} + v_c e^{j240^\circ} + v_z e^{j270^\circ}) \\ v_{xy} &= v_x + jv_y = 1/3\,(v_a + v_x e^{j150^\circ} + v_b e^{j240^\circ} \\ &\quad + v_y e^{j30^\circ} + v_c e^{j120^\circ} + v_z e^{j270^\circ}) \end{aligned} \tag{5}$$

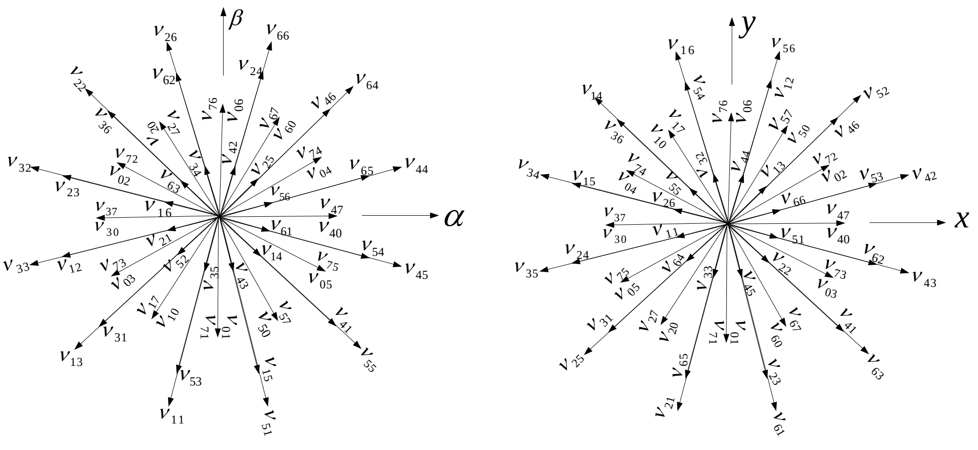

a) *α-β* plane b) *x-y* plane

Figure 5. The Distribution of Basic Space Voltage Vectors

3.2. Synthesis of the Reference Voltage Vector

Take the second sector for example to detail the TBTSB-SVPWM strategy. The relationship between reference voltage vector and four basic space voltage vectors is showed in Figure 6. where v_1, v_2, v_3, v_4 represent four basic space voltage vectors in *α-β* plane respectively, and their corresponding projections in *x-y* plane can be denoted by $v_1^{'}$, $v_2^{'}$, $v_3^{'}$, $v_4^{'}$. Amplitude values of four basic space voltage vectors both in *α-β* plane and in *x-y* plane are given in Table I and Table II.

Table 1. Amplitude Values of Four Basic Space Voltage Vectors in *α-β* Plane

Vectors	Amplitude values
v_2 , v_3	$\lvert v\rvert_{\max} = 2/3\,\mathrm{U}_{\mathrm{dc}}\cos(\pi/12)$
v_1 , v_4	$\lvert v\rvert_{\mathrm{mid}} = 2/3\,\mathrm{U}_{\mathrm{dc}}\cos(\pi/4)$

Table 2. Amplitude Values of Four Basic Space Voltage Vectors in *x-y* Plane

Vectors	Amplitude values
v_2' , v_3'	$\lvert v\rvert_{\min} = 2/3\,\mathrm{U}_{\mathrm{dc}}\cos(5\pi/12)$
v_1' , v_4'	$\lvert v\rvert_{\mathrm{mid}} = 2/3\,\mathrm{U}_{\mathrm{dc}}\cos(\pi/4)$

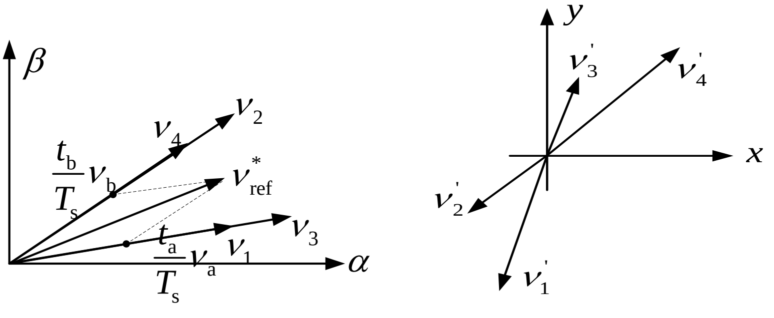

a) *α-β* plane b) *x-y* plane

Figure 6. The Relationship Between Reference Voltage Vector and Four Basic Space Voltage Vectors

Assume that the inverter switching period is T_s, application times of four basic space voltage vectors are denoted by T_1, T_2, T_3, T_4 respectively, and the application time of zero space voltage vector is T_0. The relationship between them can be described as $T_0=T_s-T_1-T_2-T_3-T_4$. According to the volt-second balance theorem, the total application time of two basic space voltage vectors in-phase can be calculated with expression (6) and expression (7).

$$t_a = \frac{\lvert v^*_{\mathrm{ref}}\rvert \sin(k\pi/6-\theta)}{\lvert v_{\max}\rvert \sin(\pi/6)} \mathrm{T_s} \tag{6}$$

$$t_b = \frac{\lvert v^*_{\mathrm{ref}}\rvert \sin(\theta-(k-1)\pi/6)}{\lvert v_{\max}\rvert \sin(\pi/6)} \mathrm{T_s} \tag{7}$$

Where k is the sector number, k=1, 2, 3…12, and the angle between the reference voltage vector and α axis is denoted by θ.

It can be seen from the Figure 6, two in-phase basic space voltage vectors in α-β plane have a phase-difference of 180 degree in x-y plane. It means that if the application times of two in-phase basic space voltage vectors are inversely proportional to amplitude values, it is possible to make the amplitude value of the reference voltage vector in x-y plane be equal to zero. Hence, inverter output phase voltage do not contain 5th and 7th harmonics and the phase voltage is pure sinusoidal.

$$\frac{|T_1|}{|T_3|}=\frac{|T_2|}{|T_4|}=\frac{|v_{max}|}{|v_{min}|}=1.367$$

Thus the application time of four basic space voltage vectors can be allocated with the following principle.

$$T_1=\frac{|v_{mid}|}{|v_{max}|+|v_{mid}|}t_a=0.4226t_a \tag{8}$$

$$T_2=\frac{|v_{max}|}{|v_{max}|+|v_{mid}|}t_b=0.5774t_b \tag{9}$$

$$T_3=\frac{|v_{max}|}{|v_{max}|+|v_{mid}|}t_a=0.5774t_a \tag{10}$$

$$T_4=\frac{|v_{mid}|}{|v_{max}|+|v_{mid}|}t_b=0.4226t_b \tag{11}$$

Since the total application time of four basic space voltage vectors is less than the inverter switching period T_s, thus it is necessary to make an adjustment to application times of four basic space voltage vectors when the total application time is more than T_s.

$$\begin{aligned}T_1'&=T_1/(T_1+T_2+T_3+T_4)\\T_2'&=T_2/(T_1+T_2+T_3+T_4)\\T_3'&=T_3/(T_1+T_2+T_3+T_4)\\T_4'&=T_4/(T_1+T_2+T_3+T_4)\end{aligned} \tag{12}$$

Consider the expression (13):

$$|v_{ref}^*|e^{j\alpha}T_s=|v_1|e^{j\pi/12}T_1+|v_2|e^{j\pi/4}T_2+|v_3|e^{j\pi/12}T_3+|v_4|e^{j\pi/4}T_4 \tag{13}$$

Substitute expression (6)-(11) into expression (13), the following relationship can be obtained:

$$|v_{ref}^*|T_se^{j\alpha}=\frac{|v_{mid}|^2+|v_{max}|^2}{|v_{max}|(|v_{max}|+|v_{mid}|)}|v_{ref}^*|T_se^{j\alpha} \tag{14}$$

Expression (14) indicates that the real amplitude of inverter output phase voltage is only 93.18% (the coefficient value of the equation on the right side) of the given reference voltage vector.

Modulation index *m* is defined as the ratio of the phase voltage fundamental peak value and one half of the DC bus voltage. For the two biggest vectors SVPWM strategy (traditional SVPWM strategy), linear modulation range can reach the inscribe cycle of dodecagon formed by twelve biggest basic space voltage vectors. Hence the maximum value of reference voltage vector is $0.622U_{dc}$, and the modulation index *m* of the two biggest vectors SVPWM strategy is 1.244, which means that the DC bus utilization is improved by 24.4%. While the modulation index *m* of the TBTSB-SVPWM strategy is only 93.18% of the modulation index of the two biggest vectors SVPWM strategy, so the modulation index *m* of the TBTSB-SVPWM strategy is 1.155, and the DC bus utilization is improved by 15.5%.

Similarly, the modulator in *x-y* plane also adopts the TBTSB-SVPWM strategy to produce *x-y* reference voltage vector required by motor2. The only difference, compared with *α-β* modulator, is that the *x-y* reference voltage vector is synthesized with four basic space voltage vectors, which consist two biggest and two second-biggest space voltage vectors in *x-y* plane.

4. Simulation Verification

In order to verify the feasibility of the proposed approach for decoupling control of the two-motor dual three-phase PMSM series-connected system, simulation experiments are performed in Matlab/Simulink. The DC bus voltage is given with 540V, and the switching frequency of inverter is 5KHz. The specific parameters of motor1 and motor2 are given in Table III. The simulation results of motor1 and motor2 under different speed/load conditions are illustrated from Figure 7 to Figure 10.

Table 3. Simulation Parameters of Two Motors

Parameters	Motor1	Motor2
Resistance of stator windings （Ω）	1.625	1.2
d-axis and q-axis inductances （mH ）	8.5	12
Permanent flux of rotor （Wb）	0.175	0.2
Moment of inertia （$K_g * m^2$）	0.085	0.1
Pole pairs	4	4

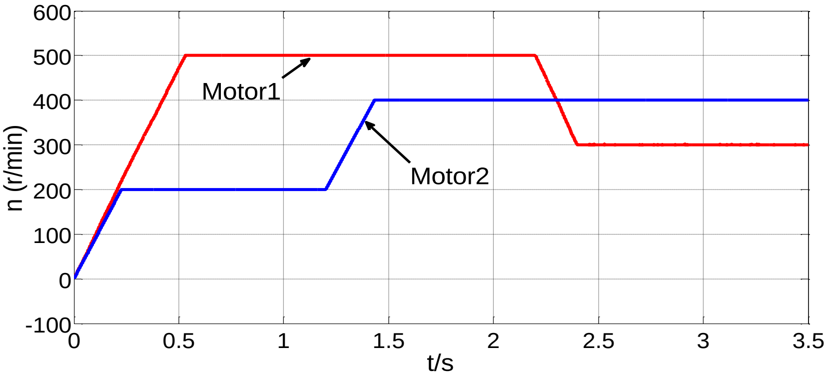

a) Speed Response Waveforms of Motor1 and Motor2

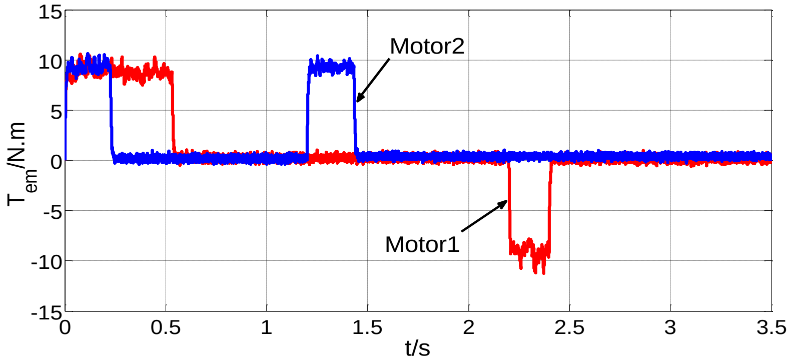

b) Electromagnetic Torque Waveforms of Motor1 and Motor2

Figure 7. Simulation Waveforms of Speed and Electromagnetic Torque Under Variable-Speed Condition

It can be seen from Figure 7 that the initial given speeds of motor1 and motor2 are 500r/min and 200r/min respectively. At the time of 1.2s, the speed of motor2 increases from 200r/min to 400r/min, and the electromagnetic torque of motor2 appears a positive pulse, which makes motor2 accelerate until the actual speed equal to the given speed of 400r/min, and then the electromagnetic torque of motor2 comes back to zero. At the time of 2.2s, the speed of motor1 decreases from 500r/min to 300r/min, and the electromagnetic torque of motor1 appears a negative pulse, which makes motor1 decelerate until the actual speed equal to the given speed of 300r/min, and then the electromagnetic torque of motor1 comes back to zero. Figure 7 also shows that in the variable-speed process of one motor, the speed /electromagnetic torque of the other motor keep unchanged.

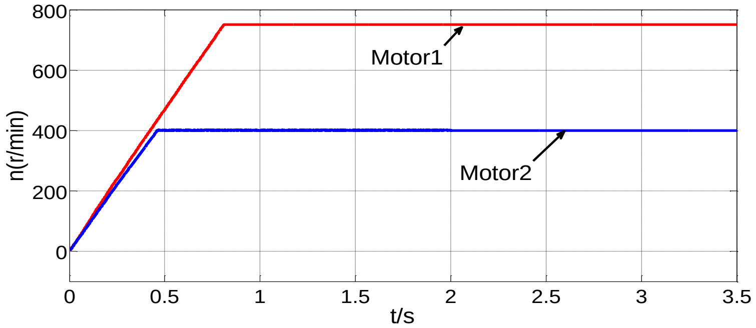

a) Speed Response Waveforms of Motor1 and Motor2

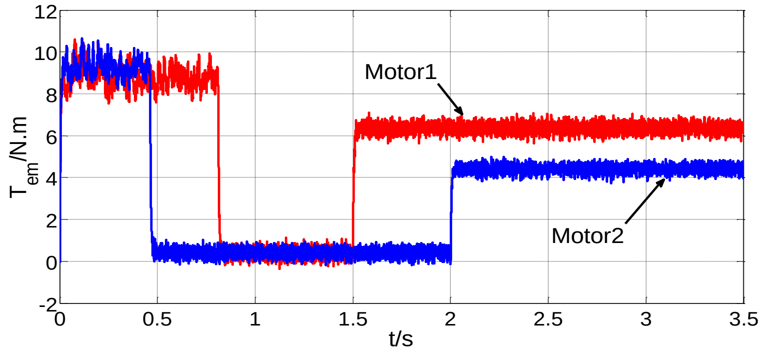

b) Electromagnetic torque waveforms of motor1 and motor2

Figure 8. Simulation Waveforms of Speed and Electromagnetic Torque Under Variable-Load Condition

It can be seen from Figure 8 that motor1 and motor2 operate at given speed of 750r/min and 400r/min respectively. At the time of 1.5s, the electromagnetic torque of motor1 increases from 0N.m to 6N.m immediately under the abrupt change of load, while the electromagnetic torque of motor2 keeps unchanged. Similarly At the time of 2s, the electromagnetic torque of motor2 increases from 0N.m to 4N.m immediately under the abrupt change of load, while the electromagnetic torque of motor1 keep unchanged.

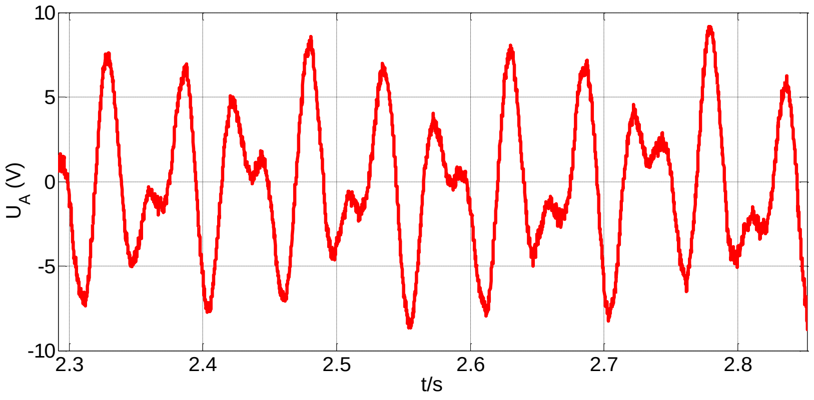

Figure 9. A-phase Voltage Waveform of Inverter in the Stationary Frame

Copyright ⓒ 2015 SERSC

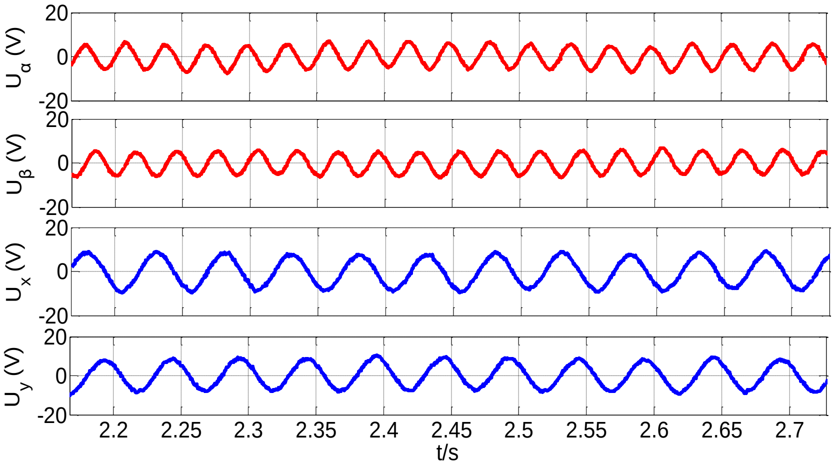

Figure 10. A-phase Voltage Waveform in *α-β* Plane and in *x-y* Plane After Decoupling Transformation

Inverter output phase voltage is also analyzed on condition that motor1 and motor2 operate at the speed of 500r/min and 300r/min respectively. A-phase voltage of inverter is shown in Fig.9. It contains two kinds of fundamental components required by each motor, so the waveforms of output phase voltage are no longer sinusoidal. However, after decoupling transformation, A-phase voltage is mapped into two 2-D planes, and the voltage waveforms of *α-β* plane and *x-y* plane are showed in Figure 10.

It can be seen from Figure 10, the period of voltage waveform in *α-β* plane is about 0.03s (33.3Hz), which corresponds to the speed of motor1 (500r/min). And the period of voltage waveform in *x-y* plane is about 0.05s (20Hz), which corresponds to the speed of motor2 (300r/min). Thus it was verified that motor1 was controlled by the *α-β* components, while motor2 was controlled by the *x-y* components. Since *α-β* plane and *x-y* plane is orthogonal, so the decoupling control of two-motor dual three-phase PMSM series-connected system can be realized through proper phase transformation.

5. Conclusion

From above analysis, when the speed/load of any motor changed, there is no impact on the speed/electromagnetic torque of the other motor in series-connected system. Thus, through proper phase transformation rules, the decoupling control of two-motor dual three-phase PMSM series-connected system can be realized, with a single supply from a six-phase VSI. Simultaneously, 5th and 7th harmonics are greatly eliminated by using the TBTSB-SVPWM technique adopted in this paper. The inverter output phase voltage only contains two kinds of voltage fundamental components required by each motor, making it possible to have the two motors operate at different conditions independently. Thus it is verified that this TBTSB-SVPWM strategy is suitable for the control of two-motor dual three-phase PMSM series-connected system. In addition, using the TBTSB-SVPWM strategy improves the DC bus voltage utilization by 15.5%, especially under the condition of limited DC bus voltage, and it can also meet the satisfaction.

Acknowledgements

All authors highly appreciate the support of the National Natural Science Foundation of China (51377168) and the Foundation of Shandong Province Science and Technology Development Planning (2011GGH20411), which made researching progress go well and ensured the achievement of the mentioned research results.

References

[1] E. Levi, R. Bojoi, F. Profumo, H. A. Toliyat and S. Williamson, "Multiphase induction motor drives-a technology status review", Journal of IET Electr Power Appl., vol. 1, no. 4, **(2007)**, pp. 489-516.

[2] M. Jones, S. N. Vukosavic and E. Levi, "Parallel Connected Multiphase Multi-drive Systems with Single Inverter Supply", Journal of IEEE Transactions on Industrial Electronics, vol. 56, no. 6, **(2009)**, pp. 2047-2057.

[3] A. Iqbal and E. Levi, "Space Vector PWM for a Five-phase VSI Supplying Two Five-phase Series-connected Machines", 12th International Power Electronics and Motion Control Conference, **(2006)**, pp. 222-227.

[4] D. Dujic, G. Grandi, M. Jones and E. Levi, "A space Vector PWM Scheme for Multi-frequency output Voltage Generation with Multiphase Voltage Source Inverter", Journal of IEEE Transactions on Industrial Electronics, vol. 55, no. 5, **(2008)**, pp. 1943-1955.

[5] E. Levi, M. Jones and A. Toliyat, "Operating Principles of a Novel Multiphase Multi-motor Vector controlled Drive", Journal of IEEE Transactions on Energy Conversion, vol. 19, no. 3, **(2004)**, pp. 508-517.

[6] E. Levi, M. Jones and A. Toliyat, "A Novel Concept of a Multiphase, Multi-motor Vector Controlled Drive System Supplied From a Single Voltage Source Inverter", Journal of IEEE Transactions on Power Electronics, vol. 19, no. 2, **(2004)**, pp. 320-335.

[7] E. Levi, M. Jones and S. N. Vukosavic, "Steady-state Modeling of Series-connected Five-Phase and Six-Phase Two Motor Drives", Journal of IEEE Transactions on Industry Applications, vol. 44, no. 5, **(2008)**, pp. 1559-1568.

[8] A. Iqbal and E. Levi, "Space Vector Modulation Schemes for a Five-phase Voltage Source Inverter", in proceeding of European Conference on Power Electronics and Applications, **(2005)**, pp. 1-12.

[9] Y. F. Zhao, T. A. Lipo, "Space vector PWM control of dual-three phase induction machine using vector space decomposition", Journal of IEEE Transactions on Industry Applications, vol. 31, no. 5, **(1995)**, pp. 1100-1109.

[10] D. Yazdani, S. A. Khajehoddin, A. Bakhshai and G. Joos, "Full Utilization of Inverter in Split phase Drives by Means of a Dual Three-phase Space Vector Classification Algorithm", Journal of IEEE Transactions on Industrial Electronics, vol. 56, no. 1, **(2009)**, pp. 120-129.

[11] A. Boglietti, R. Bojoi, A. Cavagnino and A. Tenconi, "Efficiency Analysis of PWM Inverter Fed Three-phase and Dual Three-phase High Frequency Induction Machines for low/medium Power Applications", Journal of IEEE Transactions on Industrial Electronics, vol. 55, no. 5, **(2008)**, pp. 2015-2023.

[12] D. Dujic, E. Levi and M. Jones, "Continuous PWM Techniques for Sinusoidal Voltage Generation with Seven-Phase Voltage Source Inverter", in Proceeding of Power Electronics Specialists Conference, **(2007)**, pp. 47-52.

[13] M. J. Duran, F. J. Barrero and S. L. Toral, "Multi-Dimensional Space Vectors Pulse Width Modulation Scheme for Five-phase Series-connected Two-Motor Drive", in Proceeding of Electric Machines and Drives Conference, no. 2, **(2007)**, pp. 1208-1214.

[14] A. Iqbal and S. Moinuddin, "Comprehensive Relationship between Carrier-based PWM and Space Vector PWM in a Five-phase VSI", Journal of IEEE Transactions on Power Electronics, vol. 24, no. 10, **(2009)**, pp. 2379-2390.

[15] D. Dujic, M. Jones and E. Levi, "Analysis of Output Current Ripple rms in Multiphase Drives Using Space Vector Approach", Journal of IEEE Transactions on Power Electronics, vol. 24, no. 8, **(2009)**, pp. 1926-1938.

[16] E. Levi, M. Jones, S. N. Vukosavic, A. Iqbal and H. A. Toliyat, "Modeling, control and Experimental Investigation of a five-phase series-connected Two-motor Drive with Single Inverter Supply", Journal of IEEE Trans. on Industrial Electronics, vol. 53, no. 3, **(2007)**, pp.1504-1516.

[17] S. Xue and X. H. Wen, "A novel multiphase SVPWM technique", Journal of Transactions of China Electro-technical Society, vol. 21, no. 2, **(2006)**, pp. 68-72.

[18] C. Meng, H. L. OuYang and W. H. Liu, "Space vector modulation techniques of dual Y shift 30o Permanent-magnet Synchronous Motor", Journal of Chinese Society for Electrical Engineering, vol. 30, no. 3, **(2010)**, pp. 90-98.

[19] B. Wang, Y. Wang and Z. A. Wang, "DTC strategy of permanent-magnet synchronous motor based on SVPWM techniques", Journal of Electric Machines and Control, vol. 14, no. 6, **(2010)**, pp. 45-50.

[20] J. B. Yang, G. J. Yang and T. C. Li, "Modeling and vector control of dual three-phase permanent-magnet synchronous motor", Journal of Electric Machines and Control, vol. 14, no. 6, **(2010)**, pp. 1-7.

Copyright ⓒ 2015 SERSC

Authors

Huaqiang Zhang was born in 1967. He received the B.S., M.S., and Ph.D. degrees in electrical engineering from the Harbin Institute of Technology, Harbin, China, in 1992, 1999, and 2006, respectively.

In 1992, he joined Harbin Institute of Technology as a Lecturer. Since 2009, he has been a Professor in this field. His research interests are power electronics and electrical drives and its applications, load forecasting and fault diagnosis.

Shijun Luo was born in 1990. He received the B.S. degree in electrical engineering from Harbin Institute of Technology, Harbin, China, in 2012. He is currently pursuing his M.S. degree in power electronics and electrical drives in Harbin Institute of Technology.

His main research interests are focused on power electronics and electrical drives for multiple phase motor.

Yaxin Yu was born in 1991. She received the B.S. degree in electrical engineering from Harbin Institute of Technology, Harbin, China, in 2013. She is currently pursuing her M.S. degree in power electronics and electrical drives in Harbin Institute of Technology.

Her main research interest is power electronics and electrical drives and its applications.

Lingshun Liu was born in 1969. He received the Ph.D. degree from Aeronautical and Astronautical University of Nan Jing in 2007. Now he is working in Naval Aeronautical and Astronautical University as an associate professor.

His main research interest is motor design and control.

Copyright ⓒ 2015 SERSC

Copyright ⓒ 2015 SERSC